Original Article

Diffusion tensor magnetic resonance imaging of white matter integrity in patients with HIV-associated neurocognitive disorders

Tingting Zhao[1], Jiehua Chen[1], Hang Fang[2], Danhui Fu[1], Danke Su[1], Wei Zhang[2]

[1]Guangxi Medical University, Nanning, China; [2]Department of Radiology, Affiliated Hospital of Guilin Medical University, Guilin, China

Contributions: (I) Conception and design: W Zhang, D Su; (II) Administrative support: D Su; (III) Provision of study materials or patients: T Zhao, J Chen; (IV) Collection and assembly of data: T Zhao, J Chen; (V) Data analysis and interpretation: T Zhao, J Chen, W Zhang; (VI) Manuscript writing: All authors; (VII) Final approval of manuscript: All authors.

Correspondence to: Wei Zhang. Department of Radiology, Affiliated Hospital of Guilin Medical University, Guilin, China. Email: holly2yang@126.com; Danke Su. Guangxi Medical University, Nanning 530021, China. Email: sudanke33@sina.com.

Background: This study investigated the efficacy and neurotoxicity of highly active antiretroviral therapy (HAART) by evaluating white matter (WM) injury using diffusion tensor magnetic resonance imaging (DTI) in patients with human immunodeficiency virus (HIV)-associated neurocognitive disorders (HAND).

Methods: Forty-six patients with HAND underwent DTI before and every six months during HAART treatment. DTI data, including fractional anisotropy (FA) and mean diffusivity (MD) values of structural WM before and after HAART, were compared. The relationship between DTI values and plasma viral loads was tested. MD was more sensitive than FA for evaluating WM injury in HAND-positive patients.

Results: Following 12 months of HAART, increased MD values (compared to 6 months of HAART) were observed in the right temporal lobe, right parietal lobe, right occipital lobe, right anterior limb of the internal capsule, right lenticular nucleus, the right cerebral peduncle, left caudate nucleus, left dorsal thalamus, and left posterior limb of the internal capsule. MD values in the left genu of the internal capsule (r=0.350, P=0.017) and left corona radiata (r=0.338, P=0.021) were positively correlated with plasma viral loads.

Conclusions: DTI may be useful for assessing the efficacy and neurotoxicity of HAART in HAND-positive patients. Starting HAART may halt WM injury; however, prolonged HAART could worsen WM injury, highlighting the importance of optimal HAART duration.

Keywords: Human immunodeficiency virus (HIV); white matter (WM); diffusion tensor imaging; highly active antiretroviral therapy (HAART)

Submitted Aug 18, 2020. Accepted for publication Oct 13, 2020.
doi: 10.21037/atm-20-6342
View this article at: http://dx.doi.org/10.21037/atm-20-6342

Introduction

The incidence of human immunodeficiency virus (HIV) infection shows regional variations (1). Guangxi has the second-highest prevalence of patients with HIV and mortality because of HIV infection in China (2). The data from the China Centers for Disease Control Epidemic Information System reported that Guangxi had 85,576 cases of HIV infection and AIDS and 49,109 cases of death following HIV infection in December 2018. HIV penetrates the central nervous system (CNS) at the early stages of infection, even in the pre-acquired immune deficiency syndrome phase (3), and leads to inflammation in the brain. Ongoing CNS inflammation may lead to cognitive and behavioral abnormalities, which are called HIV-associated neurocognitive disorders (HAND) (4). Advancements in

highly active antiretroviral therapy (HAART) has led to a profound decrease in the morbidity and mortality of HIV-infected individuals (5,6). However, patients with HIV continue to experience HAND (7,8). This cognitive dysfunction can affect daily function (9) and increase the risk of death in patients with HIV (10). Although research has suggested HAART cannot reverse previous damage, recent studies have reported that effective HAART could prevent the progression of CNS injury (11,12). However, it is possible that the prolonged use of HAART may also induce neurotoxicity (13,14).

It is often challenging to diagnose HAND and post-HAART neurocognitive functions with a neuropsychological (NP) battery of tests because of differences in language and cultural environments (2,15). Also, NP tests are tedious and cannot be performed by patients with physical disabilities (16).

Diffusion tensor imaging (DTI) is an imaging modality that can be used for the quantitative assessment of brain white matter (WM) abnormalities associated with the initial stages of HIV (17-19). DTI tests the directional nature of water diffusion through cellular structures in the brain WM and shows brain integrity with fractional anisotropy (FA) and mean diffusivity (MD) (20-22). FA and MD can supply complementary quantitative information on WM structure; FA reflects axonal microstructural integrity, and MD reflects the average diffusion in tissue (23). Although some results have been controversial (24), most studies have shown that FA was decreased, and MD was increased in different WM regions of HIV-infected patients (17-22). Stubbe-Drger *et al.* (25) found that there were no statistical differences in FA between patients taking HAART and those who not. Patients with HAND had significant FA reduction relative to patients without HAND. However, the primary focus of the earlier DTI studies of HAND has been the differences in WM structure between HIV-infected individuals and non-infected controls. To our knowledge, the causative relationship between the neurotoxicity of HAART and neurocognitive function impairment in patients with HAND individuals is still uncertain.

Therefore, it is essential to investigate the WM integrity of patients with HAND by assessing differences in DTI values and plasma viral load following 6 and 12 months of HAART. The purpose of this study was to test the efficacy and neurotoxicity of HAART in HIV-infected individuals using DTI. The NP battery of tests was assessed as secondary endpoints. We present the following article in accordance with the MDAR reporting checklist (available at http://dx.doi.org/10.21037/atm-20-6342).

Methods

Patients

We randomly selected 48 patients (31 men and 17 women; mean age, 43.96±13.21 years) with HAND who underwent magnetic resonance imaging (MRI) at the Affiliated Tumor Hospital of Guangxi Medical University and received HAART at the Fourth People's Hospital of Nanning from January 2017 to January 2018. The follow-up period was up to 12 months of HAART. Two neurologists/psychiatrists confirmed HAND with 5 years of relevant clinical experience with AIDS-related nervous system symptoms. The symptoms were assessed according to the diagnostic criteria set up by the American Academy of Neurology (Grant 2008) to support a uniform standard throughout the diagnostic process. Following these criteria (2,9,15), patients with comorbid conditions that could affect cognitive or daily functioning were excluded from the study. The values of plasma viral loads were with the normal ranges used at our institution. All procedures performed in this study involving human participants were in accordance with the Declaration of Helsinki (as revised in 2013). This study was approved by the Ethics Committee of Wuming Hospital of Guangxi Medical University (No. FSWM2020-126). All patients signed informed consent forms.

Image acquisition

All DTI scans of the brain were acquired using a 1.5-T scanner (Avanto, Siemens, Erlangen, Germany) with an 8-channel phased-array head coil and equipped with the following parameters: axial T_1-weighted sequence [repetition time (TR) =199 ms, echo time (TE) =4.76 ms], axial T_2-weighted sequence (TR =4,000 ms, TE =105 ms), axial fluid attenuation inversion recovery (TR =7,600 ms, TE =92 ms), field of view (FOV) =210 mm, matrix =384×192, section thickness =6 mm, intersection gaP =2 mm, and flip angle =70°. A transverse diffusion tensor single-shot echo-planar scan was performed with bipolar diffusion gradients applied along 20 non-collinear and non-coplanar directions (b0 =0 and b1 =1,000 s/mm^2) using the following parameters: TR =5,000 ms, TE =97 ms; FOV =210 mm; matrix =128×128, flip angle =90°, total acquisition 35 slices with 4 mm thickness, and 1 gap.

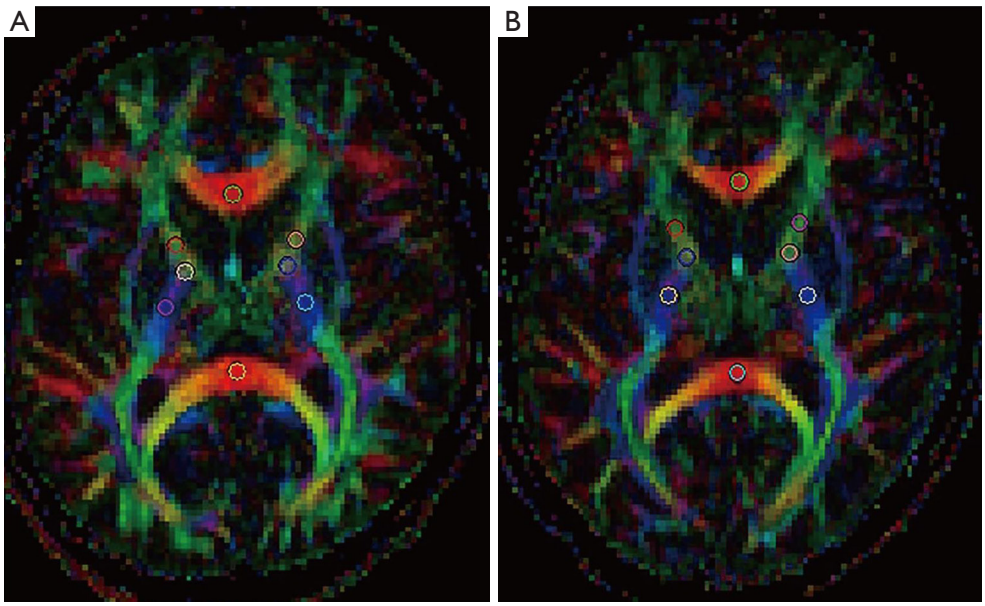

Figure 1 Region of interests of a healthy person (A) and patients with human immunodeficiency virus-associated neurocognitive disorders (B).

DTI analysis

All DTI data were processed with the functional MRI of the brain software library of Siemens Company's ADW42 workstation. All images were processed using motion correction to stop the misregistration caused by slight movements during scanning. Gaussian smoothing was applied to remove the background noise without the loss of valuable information. The software generated three-dimensional color DTI, FA, and MD maps. We identified 30 primary regions of interest (ROIs) of WM tracts to investigate the WM characteristics of the whole brain before and after HAART, including the WM of the frontal lobe, temporal lobe, parietal lobe, occipital lobe, dorsal thalamus, anterior limb of the internal capsule, posterior limb of the internal capsule, genu of the internal capsule, genu of the corpus callosum, the body of the corpus callosum, splenium of the corpus callosum, corona radiata, lenticular nucleus, caudate nucleus, cerebral peduncles, and middle cerebellar peduncle. ROIs were manually drawn to extract 6–9-mm^2 circles while excluding areas of grey matter or cerebrospinal fluid (CSF). The area of the ROI selected was less than the area of the corresponding brain WM structure (*Figure 1*). ROIs were repeatedly measured three times, and the mean FA and MD in each WM tract were calculated for each patient.

NP tests

The 14 NP tests are described in our earlier studies (2).

Statistical analysis

Statistical analyses were performed using SPSS version 22.0 (IBM Corp., Armonk, NY, USA) statistical software. These results were expressed as mean ± standard deviation. To investigate changes in WM injury before and after HAART, we conducted repeated measures, univariate analysis of variance, and multiple comparisons, using Bonferroni correction, which was performed in the three groups. Bivariate correlation analyses were used to determine the correlation between plasma viral loads and both DTI values and NP test results. For all analyses, $P<0.05$ was considered statistically significant.

Results

Patient characteristics

Forty-six patients (29 men and 17 women) with HAND completed the follow-up period, with a loss to the follow-up rate of 4.2%. Of the 46 patients, 14 patients had received senior high school education or above, 32 were

Table 1 Demographic characteristics of study participants

Demographic characteristics	N (constituent ratio %)
Sex	
Male	29 (63.04)
Female	17 (36.96)
Age (in years)	
20–29	9 (19.56)
30–39	5 (10.87)
40–49	15 (32.61)
50–59	12 (26.09)
60–65	5 (10.87)
Ethnicity	
Han	19 (41.30)
Zhuang	25 (54.35)
Yao	2 (4.35)
Education	
Primary school or less	12 (26.09)
Junior high school or less	20 (43.48)
High school or higher	14 (30.43)
Marital status	
Married	32 (69.56)
Unmarried	10 (21.74)
Divorced	2 (4.35)
Widowed	2 (4.35)
Profession	
Farmer	17 (39.95)
Staff	10 (21.74)
Migrant laborer	10 (21.74)
Health personnel	2 (4.35)
Unemployed	5 (10.87)
Other	2 (4.35)
History of drug abuse	
None	37 (80.44)
Ever	9 (19.56)

married, and 37 had no history of drug abuse. Demographic characteristics are shown in *Table 1*.

The FA values of WM tracts before and after HAART

We observed changes in the FA values of WM tracts after HAART in the follow-up period (*Table 2*, *Figure 2*). HAND-positive patients exhibited significantly higher FA values in the right temporal lobe and right lenticular nucleus and lowered FA in the right caudate nucleus and right dorsal thalamus after six months of HAART than FA values before HAART. Further, FA values are higher in the right caudate nucleus and lower in the right lenticular nucleus and right dorsal thalamus after 12 months of HAART than after 6 months of therapy (P<0.05).

The MD values of WM tracts before and after HAART

We also observed changes in the MD values of WM tracts after HAART in the follow-up period (*Table 3*, *Figure 3*). HAND-positive patients exhibited significantly lower MD in the right temporal lobe, right parietal lobe, right lenticular nucleus, the right cerebral peduncle, left caudate nucleus, left dorsal thalamus, and genu of the corpus callosum and higher MD in the right dorsal thalamus after 6 months of HAART than before HAART. HAND-positive patients exhibited significantly higher MD in the right temporal lobe, right occipital lobe, right anterior limb of the internal capsule, right dorsal thalamus, and lower MD in the left genu of the internal capsule after 12 months of HAART than before HAART. MD values were higher in the right temporal lobe, right parietal lobe, right occipital lobe, right anterior limb of the internal capsule, right lenticular nucleus, the right cerebral peduncle, left caudate nucleus, left dorsal thalamus, and left posterior limb of the internal capsule and lower in the left lenticular nucleus after 12 months of HAART than after 6 months of therapy (P<0.05).

Correlations between DTI metrics and plasma viral loads before and after HAART

There was a strong negative correlation between plasma loads and HAART in HIV-infected patients (P<0.05). Specifically, as the treatment progressed, the plasma loads decreased (*Figure 4*). There was a significant difference in plasma viral loads before and after six months of HAART (before, 3.696±0.707 copies/mL. Also, after six months, the levels were 2.159±0.444 copies/mL, P<0.001). Further, the plasma viral loads were significantly lower after 12 months of HAART (1.430±0.337 copies/mL) than before HAART (P<0.001) and after 6 months of HAART (P<0.001). The FA values of the main WM tracts were not statistically correlated with plasma viral loads; however, the MD values in the left genu of the internal capsule (r=0.350, P=0.017) and left corona radiata (r=0.338, P=0.021) were positively correlated with plasma viral loads before HAART and after

Table 2 The FA values of 46 study participants before and after HAART

Region	Group	FA	95% CI	F	P[a]
Frontal lobe_R	1	0.445±0.033	0.436–0.455	0.384	0.682
	2	0.451±0.036	0.440–0.461		
	3	0.450±0.032	0.441–0.460		
Frontal lobe_L	1	0.438±0.029	0.430–0.447	1.702	0.188
	2	0.430±0.021	0.423–0.436		
	3	0.438±0.028	0.429–0.446		
Temporal lobe_R	1	0.396±0.029	0.388–0.405	13.322	0.000
	2	0.426±0.037	0.415–0.437*		
	3	0.434±0.041	0.422–0.447*		
Temporal lobe_L	1	0.452±0.037	0.440–0.463	0.432	0.607
	2	0.447±0.050	0.432–0.462		
	3	0.445±0.011	0.441–0.448		
Parietal lobe_R	1	0.527±0.029	0.518–0.535	4.559	0.013
	2	0.536±0.030	0.527–0.545		
	3	0.545±0.031	0.536–0.554		
Parietal lobe_L	1	0.530±0.022	0.524–0.537	0.088	0.817
	2	0.531±0.016	0.526–0.536		
	3	0.534±0.073	0.512–0.556		
Occipital lobe_R	1	0.218±0.036	0.208–0.229	1.932	0.160
	2	0.207±0.037	0.196–0.218		
	3	0.218±0.027	0.210–0.226		
Occipital lobe_L	1	0.206±0.019	0.200–0.211	2.546	0.084
	2	0.202±0.024	0.195–0.209		
	3	0.211±0.017	0.206–0.216		
Genu of the corpus callosum	1	0.800±0.034	0.790–0.810	0.702	0.498
	2	0.799±0.035	0.789–0.810		
	3	0.792±0.034	0.782–0.802		
Splenium of the corpus callosum	1	0.856±0.094	0.828–0.884	1.530	0.224
	2	0.841±0.084	0.816–0.866		
	3	0.867±0.016	0.862–0.872		
Body of the corpus callosum_R	1	0.809±0.040	0.797–0.821	2.088	0.130
	2	0.794±0.038	0.783–0.805		
	3	0.807±0.040	0.795–0.819		

Table 2 (*continued*)

Table 2 (*continued*)

Region	Group	FA	95% CI	F	P[a]
Body of the corpus callosum_L	1	0.818±0.375	0.706–0.929	0.197	0.822
	2	0.775±0.300	0.686–0.864		
	3	0.809±0.347	0.706–0.913		
Anterior limb of the internal capsule_R	1	0.614±0.035	0.604–0.625	1.510	0.226
	2	0.612±0.046	0.598–0.626		
	3	0.626±0.041	0.614–0.638		
Anterior limb of the internal capsule_L	1	0.615±0.089	0.588–0.641	0.883	0.369
	2	0.619±0.010	0.616–0.622		
	3	0.630±0.038	0.619–0.642		
Posterior limb of the internal capsule_R	1	0.712±0.029	0.703–0.721	1.299	0.278
	2	0.701±0.035	0.690–0.711		
	3	0.707±0.036	0.697–0.718		
Posterior limb of the internal capsule_L	1	0.724±0.024	0.717–0.731	0.031	0.970
	2	0.725±0.027	0.717–0.733		
	3	0.725±0.021	0.719–0.731		
Genu of the internal capsule_R	1	0.653±0.044	0.640–0.666	0.708	0.495
	2	0.641±0.042	0.629–0.654		
	3	0.645±0.044	0.632–0.658		
Genu of the internal capsule_L	1	0.656±0.039	0.644–0.667	0.365	0.695
	2	0.649±0.041	0.637–0.662		
	3	0.650±0.040	0.638–0.662		
Lenticular nucleus_R	1	0.233±0.026	0.225–0.241	26.254	0.000
	2	0.269±0.020	0.263–0.275*		
	3	0.243±0.024	0.236–0.250#		
Lenticular nucleus_L	1	0.242±0.114	0.208–0.276	0.019	0.964
	2	0.245±0.029	0.237–0.254		
	3	0.245±0.099	0.216–0.275		
Caudate nucleus_R	1	0.190±0.049	0.176–0.205	5.017	0.017
	2	0.170±0.022	0.163—0.176*		
	3	0.186±0.017	0.181–0.191#		
Caudate nucleus_L	1	0.201±0.024	0.194–0.208	7.113	0.001
	2	0.189±0.022	0.183–0.196		
	3	0.183±0.020	0.178–0.189*		

Table 2 (*continued*)

Table 2 (*continued*)

Region	Group	FA	95% CI	F	P[a]
Dorsal thalamus_R	1	0.300±0.015	0.295–0.305	9.301	0.000
	2	0.304±0.014	0.300–0.308		
	3	0.291±0.019	0.285–0.296*#		
Dorsal thalamus_L	1	0.298±0.014	0.293–0.302	4.426	0.020
	2	0.289±0.009	0.287–0.292*		
	3	0.290±0.019	0.285–0.296		
Corona radiata_R	1	0.414±0.024	0.407–0.421	1.028	0.362
	2	0.419±0.018	0.414–0.424		
	3	0.420±0.021	0.413–0.426		
Corona radiata_L	1	0.431±0.071	0.410–0.452	0.082	0.899
	2	0.429±0.054	0.413–0.445		
	3	0.427±0.022	0.420–0.433		
Cerebral pedunculus_R	1	0.553±0.032	0.543–0.562	2.310	0.105
	2	0.538±0.036	0.527–0.549		
	3	0.548±0.036	0.538–0.559		
Cerebral pedunculus_L	1	0.538±0.017	0.532–0.543	1.901	0.174
	2	0.558±0.087	0.532–0.583		
	3	0.542±0.008	0.539–0.544		
Middle cerebellar peduncle_R	1	0.713±0.032	0.704–0.723	0.503	0.568
	2	0.663±0.285	0.578–0.747		
	3	0.707±0.363	0.599–0.815		
Middle cerebellar peduncle_L	1	0.724±0.045	0.711–0.738	2.580	0.081
	2	0.705±0.036	0.695–0.716		
	3	0.717±0.046	0.703–0.731		

Data are mean values ± standard deviation. P[a] values for comparison among three groups (before HAART, after 6 months of HAART, and after 12 months of HAART). *, P<0.05 (compared with before HAART); #, P<0.05 (compared with 6 months of HAART). Group 1, without HAART; Group 2, after six months of HAART; Group 3, after 12 months of HAART. CI, confidence interval; FA, fractional anisotropy; HAART, highly active antiretroviral therapy; L, left; R, right.

12 months of HAART.

Analytical comparison of NP test results before and after HAART

The NP test scores of HAND-positive patients showed significantly better in all the testing methods except for the Wisconsin Card Sorting Test classification after 6 months of HAART than before HAART. The scores were worse in wood puzzles, immediate visual memory, delayed visual memory, Stroop C, Stroop CW, non-vocabulary fluency, and concept fluency test after 12 months of HAART than after six months of therapy (P<0.05) (*Table 4*). The digit span test value was positively correlated with plasma viral loads before HAART and after 12 months of HAART (r=0.352, P=0.016).

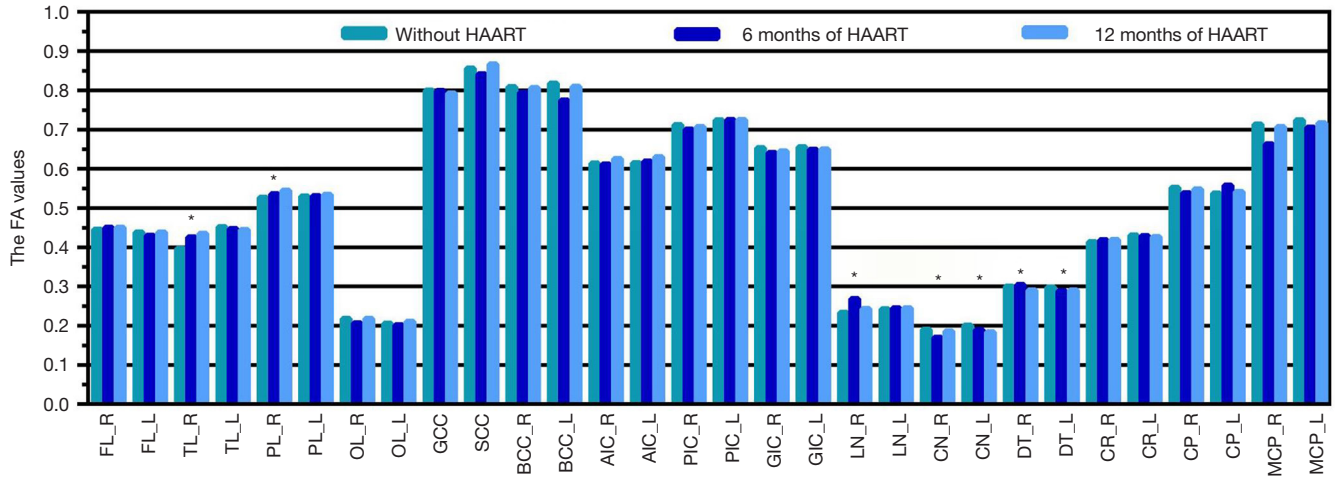

Figure 2 The FA values of WM tracts before and after HAART. *, P<0.05. HAART, highly active antiretroviral therapy; AIC, anterior limb of the internal capsule; BCC, the body of the corpus callosum; CN, caudate nucleus; CP, cerebral peduncle; CR, corona radiata; DT, dorsal thalamus; FA, fractional anisotropy; FL, frontal lobe; GCC, genu of the corpus callosum; GIC, genu of the internal capsule; HAART, highly active antiretroviral therapy; L, left; LN, lenticular nucleus; MCP, middle cerebellar peduncle; OL, occipital lobe; PIC, posterior limb of the internal capsule; PL, parietal lobe; R, right; SCC, splenium of the corpus callosum; TL, temporal lobe WM, white matter.

Discussion

The current study investigated the efficacy and neurotoxicity of HAART by evaluating the extent of brain WM injury using DTI in patients with HAND. Results from this study showed that changes in MD in WM tracts were more extensive than changes in FA in WM tracts. Unlike the FA values, the MD values were statistically correlated with plasma viral loads. Like earlier studies, our results showed that changes in the MD values were more commonly observed than changes in the FA values (17,19,20).

DTI measures four parameters, including FA, axial diffusivity (AD), MD, and radial diffusivity (RD). In this study, we focused only on FA and MD, while AD and RD were not calculated. However, FA and MD are influenced by AD and RD. FA can reflect the microstructural integrity of axons through the deviation of water motion (23), and studies have suggested that changes in RD may induce FA abnormalities (20,23,26). RD is known to be related to the destruction of myelin integrity and is a marker for demyelination induced by inflammation (27-30). MD may reflect cell degeneration and membrane density, though the speed of water molecule diffusion (31,32). MD abnormalities have been attributed primarily to AD changes (20), and increased AD is a marker of chronic axonal damage (31,32). Our results showed that MD was more sensitive than FA in evaluating WM injury in HAND-positive patients. These findings showed that axonal injury might exist before the integrity of myelin is disrupted. However, it is unclear if axonal damage can trigger demyelination. Therefore, the relationship between axonal and myelin damage should be determined in future HAND pathology studies.

The detrimental effects on WM structure and function following the prolonged use of HAART are still controversial (33-36). Therefore, our study tested the correlation between DTI metrics and HAART, which ultimately reflects the changes in the WM microstructure. Our results supply evidence HAART may prevent the progression of WM injury, at least in the short run. The early implementation of HAART in HIV-infected patients helps suppress viral replication in the plasma and CSF (8). However, the changes in the DTI parameters of the right caudate nucleus and right dorsal thalamus observed in our study are difficult to explain. These findings might be explained by the ability of HIV to penetrate the blood-CSF barrier and accumulate in the CSF (3). Drugs must first cross the blood-brain barrier (BBB) to enter the CNS, and an intact BBB causes this entry to be challenging. These results may also be because of differences in the cognitive status and disease duration of different WM areas in patients with HAND. Our findings suggest that

Table 3 The MD values of 46 study participants before and after HAART

Region	Group	MD	95% CI	F	P[a]
Frontal lobe_R	1	0.754±0.047	0.740–0.768	1.407	0.250
	2	0.741±0.030	0.732–0.750		
	3	0.753±0.041	0.741–0.765		
Frontal lobe_L	1	0.753±0.042	0.741–0.765	0.048	0.954
	2	0.754±0.041	0.741–0.766		
	3	0.751±0.040	0.739–0.763		
Temporal lobe_R	1	0.798±0.025	0.790–0.805	11.908	0.000
	2	0.781±0.034	0.771–0.791*		
	3	0.818±0.048	0.804–0.832*#		
Temporal lobe_L	1	0.776±0.028	0.767–0.784	2.348	0.131
	2	0.742±0.042	0.730–0.755		
	3	0.802±0.222	0.736–0.868		
Parietal lobe_R	1	0.794±0.012	0.791–0.798	10.297	0.001
	2	0.767±0.035	0.757–0.778*		
	3	0.814±0.075	0.791–0.836#		
Parietal lobe_L	1	0.779±0.060	0.761–0.797	1.190	0.298
	2	0.765±0.019	0.760–0.771		
	3	0.775±0.034	0.765–0.785		
Occipital lobe_R	1	0.774±0.040	0.762–0.786	17.215	0.000
	2	0.757±0.039	0.746–0.769		
	3	0.800±0.025	0.793–0.808*#		
Occipital lobe_L	1	0.787±0.026	0.780–0.795	0.286	0.720
	2	0.788±0.028	0.779–0.796		
	3	0.792±0.039	0.780–0.803		
Genu of the corpus callosum	1	0.793±0.030	0.784–0.802	8.437	0.000
	2	0.761±0.050	0.746–0.776*		
	3	0.779±0.035	0.769–0.789		
Splenium of the corpus callosum	1	0.749±0.047	0.735–0.763	0.755	0.473
	2	0.741±0.041	0.729–0.753		
	3	0.752±0.041	0.740–0.765		
Body of the corpus callosum_R	1	0.847±0.062	0.829–0.866	1.557	0.216
	2	0.828±0.051	0.813–0.844		
	3	0.844±0.051	0.829–0.859		

Table 3 (*continued*)

Table 3 (*continued*)

Region	Group	MD	95% CI	F	P[a]
Body of the corpus callosum_L	1	0.846±0.041	0.834–0.858	3.031	0.053
	2	0.834±0.032	0.824–0.843		
	3	0.829±0.036	0.818–0.839		
Anterior limb of the internal capsule_R	1	0.761±0.038	0.750–0.772	5.898	0.007
	2	0.769±0.028	0.760–0.777		
	3	0.781±0.011	0.778–0.784*#		
Anterior limb of the internal capsule_L	1	0.770±0.031	0.761–0.779	0.107	0.899
	2	0.769±0.028	0.760–0.777		
	3	0.767±0.031	0.758–0.776		
Posterior limb of the internal capsule_R	1	0.740±0.022	0.734–0.747	2.716	0.081
	2	0.727±0.026	0.719–0.735		
	3	0.740±0.040	0.728–0.751		
Posterior limb of the internal capsule_L	1	0.726±0.040	0.714–0.738	7.136	0.001
	2	0.712±0.034	0.701–0.722		
	3	0.739±0.021	0.733–0.745#		
Genu of the internal capsule_R	1	0.759±0.016	0.755–0.764	2.405	0.106
	2	0.736±0.073	0.714–0.757		
	3	0.758±0.063	0.739–0.776		
Genu of the internal capsule_L	1	0.761±0.039	0.749–0.772	3.341	0.040
	2	0.748±0.041	0.736–0.760		
	3	0.739±0.041	0.727–0.752*		
Lenticular nucleus_R	1	0.781±0.040	0.769–0.793	7.159	0.002
	2	0.759 ±0.033	0.749–0.769*		
	3	0.783±0.021	0.777–0.789#		
Lenticular nucleus_L	1	0.752±0.051	0.737–0.767	3.918	0.023
	2	0.777±0.052	0.761–0.792		
	3	0.751±0.047	0.738–0.765#		
Caudate nucleus_R	1	0.758±0.039	0.746–0.770	1.579	0.212
	2	0.751±0.036	0.740–0.761		
	3	0.763±0.020	0.757–0.769		
Caudate nucleus_L	1	0.773±0.040	0.761–0.785	6.729	0.005
	2	0.742±0.023	0.735–0.749*		
	3	0.766±0.056	0.750–0.783#		

Table 3 (*continued*)

Table 3 (*continued*)

Region	Group	MD	95% CI	F	P[a]
Dorsal thalamus_R	1	0.717±0.040	0.705–0.729	63.418	0.000
	2	0.804±0.052	0.789–0.819*		
	3	0.791±0.032	0.781–0.800*		
Dorsal thalamus_L	1	0.770±0.020	0.764–0.776	14.768	0.000
	2	0.734±0.033	0.724–0.743*		
	3	0.762±0.044	0.749–0.776#		
Corona radiata_R	1	0.769±0.017	0.764–0.774	1.655	0.197
	2	0.752±0.073	0.730–0.774		
	3	0.750±0.059	0.733–0.767		
Corona radiata_L	1	0.758±0.030	0.749–0.767	1.295	0.279
	2	0.745±0.037	0.734–0.756		
	3	0.752±0.041	0.740–0.764		
Cerebral pedunculus_R	1	0.790±0.027	0.782–0.798	14.533	0.000
	2	0.764±0.035	0.754–0.775*		
	3	0.810±0.060	0.792–0.828#		
Cerebral pedunculus_L	1	0.791±0.041	0.779–0.804	1.996	0.142
	2	0.805±0.033	0.795–0.815		
	3	0.797±0.033	0.787–0.807		
Middle cerebellar peduncle_R	1	0.697±0.067	0.677–0.717	1.271	0.279
	2	0.697±0.031	0.688–0.706		
	3	0.710±0.021	0.704–0.717		
Middle cerebellar peduncle_L	1	0.696±0.053	0.680–0.712	0.776	0.464
	2	0.704±0.048	0.690–0.718		
	3	0.707±0.035	0.697–0.718		

Data are mean values ± standard deviation. P[a] values for comparison among three groups (before HAART, after 6 months of HAART, and after 12 months of HAART). *, P<0.05 (compared with before HAART); #, P<0.05 (compared with 6 months of HAART); Group 1, without HAART; Group 2, 6 months of HAART; and Group 3, 12 months of HAART. CI, confidence interval; HAART, highly active antiretroviral therapy; MD, mean diffusivity; L, left, R, right.

HAART may prevent the progression of CNS injury, which emphasizes the importance of prompt treatment in infected individuals. As secondary endpoints, the results of NP tests also confirm this view, HAART improves the WM, at least in the short run.

The MD values in the left genu of the internal capsule and left corona radiata are positively correlated with plasma viral loads, which might be because of the selective involvement of WM in patients with HAND. Specifically, the virus penetrates vulnerable regions of the BBB to infect and activate local CNS immune cells. Studies have shown that periventricular WM, especially corona radiata, are more vulnerable to viral invasion and neuroinflammation in HIV-infected individuals (18,31,37-39). Higher plasma viral loads have been associated with higher MD values in the left genu of the internal capsule and left corona radiata and increased activity and replication of HIV, which may lead to viral accumulation in the CSF. Therefore, we used DTI

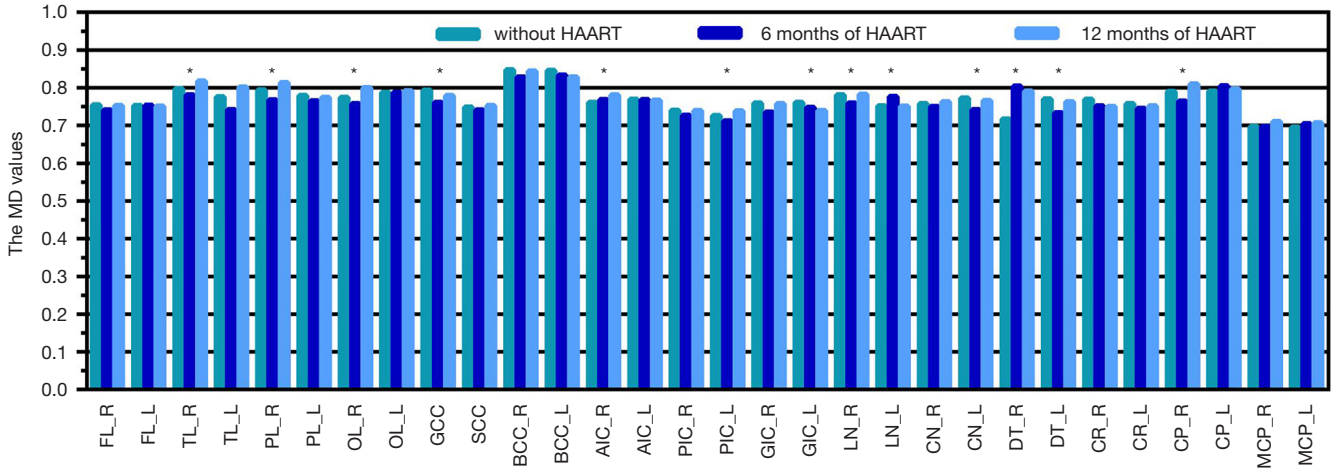

Figure 3 The MD values of WM tracts before and after HAART. *, P<0.05. HAART, highly active antiretroviral therapy; AIC, anterior limb of the internal capsule; BCC, the body of the corpus callosum; CN, caudate nucleus; CP, cerebral peduncle; CR, corona radiata; DT, dorsal thalamus; FL, frontal lobe; GCC, genu of the corpus callosum; GIC, genu of the internal capsule; HAART, highly active antiretroviral therapy; L, left; LN, lenticular nucleus; MCP, middle cerebellar peduncle; MD, mean diffusivity; OL, occipital lobe; PIC, posterior limb of the internal capsule; PL, parietal lobe; R, right; SCC, splenium of the corpus callosum; TL, temporal lobe WM, white matter.

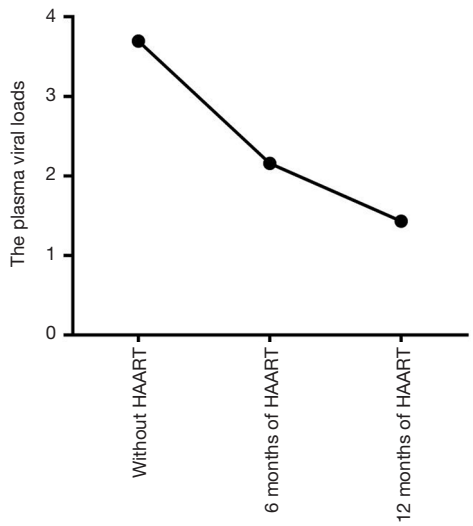

Figure 4 The plasma viral loads before and after HAART. HAART, highly active antiretroviral therapy.

as a measurement of neuronal injury to monitor CSF viral loads. However, further investigation must characterize the relationship between DTI values and CSF viral loads.

After 12 months of HAART, the MD values in the right temporal lobe, right parietal lobe, right occipital lobe, right anterior limb of the internal capsule, right lenticular nucleus, right cerebral peduncle, left caudate nucleus, left dorsal thalamus, and left posterior limb of the internal capsule, which is significantly higher than the MD values after six months of HAART. The scores were worse for the wood puzzle, immediate visual memory, delayed visual memory, Stroop C, Stroop CW, non-vocabulary fluency, and the concept fluency test after 12 months of HAART than after six months of therapy. These results prove that damage to the WM of these brain regions progressed in virologically well-controlled patients with HAND after HAART. It is neurotoxicity damage to the nerve from HAART that can lead to changes in DTI parameters. Therefore, we hypothesize that the side effects of HAART caused these results. However, further studies are needed to resolve this issue.

Limitations in this study included a small size sample and short follow-up duration. However, our DTI findings after six months of HAART were like earlier reports, which support the reliability of these results. Further, we focused only on FA and MD in the current study; AD and RD were omitted. However, studies have reported that changes induce FA changes primarily in RD (20,23,26) and MD changes are mainly attributed to AD alterations (20). Therefore, we believe our results suffice to prove injury to the WM. Data on the lifestyle of participants is not collected, and different lifestyle factors, including alcohol

Table 4 The neuropsychological tests of 46 study participants before and after HAART

Testing method	Group	Scores	95% CI	F	P[a]
Digit symbol test	1	47.91±6.56	45.96–49.86	8.949	0.000
	2	52.57±6.95	50.50–54.63*		
	3	50.96±6.08	49.15–52.76*		
Trail making test	1	78.63±16.00	73.88–83.38	1.931	0.165
	2	73.09±15.77	68.41–77.77*		
	3	72.89±18.10	67.52–78.27		
Arithmetic score	1	7.83±1.10	7.50–8.15	31.803	0.000
	2	10.94±2.40	10.22–11.65*		
	3	10.20±2.33	9.50–10.89*		
Digit span test	1	10.30±2.56	9.54–11.07	9.847	0.000
	2	12.48±1.52	12.03–12.93*		
	3	11.96±3.18	11.01–12.90*		
Wood puzzle	1	18.61±1.97	18.02–19.19	103.849	0.000
	2	28.35±2.85	27.50–29.19*		
	3	21.96±4.47	20.63–23.26*#		
Immediate visual memory	1	9.39±1.20	9.04–9.75	64.032	0.000
	2	12.59±1.34	12.19–12.99*		
	3	11.35±1.35	10.95–11.75*#		
Visual delayed memory	1	6.17±1.00	5.88–6.47	134.382	0.000
	2	10.96±1.19	10.60–11.31*		
	3	8.00±1.84	7.45–8.55*#		
Stroop C	1	88.91±16.89	83.90–93.93	8.175	0.001
	2	77.96±18.08	72.59–83.33*		
	3	86.80±18.38	81.35–92.26#		
Stroop CW	1	106.59±19.66	100.75–112.43	15.175	0.000
	2	92.54±19.40	86.78–98.30*		
	3	100.00±17.90	94.68–105.32#		
Vocabulary fluency	1	8.98±0.98	8.69–9.27	121.347	0.000
	2	16.76±2.09	16.14–17.38*		
	3	11.65±3.37	10.65–12.65*#		
Non-vocabulary fluency	1	9.44±0.89	9.17–9.70	138.629	0.000
	2	17.65±1.93	17.08–18.23*		
	3	12.07±3.42	11.05–13.08*#		

Table 4 (*continued*)

Table 4 (*continued*)

Testing method	Group	Scores	95% CI	F	P[a]
Concept fluency test	1	9.57±0.98	9.27–9.86	61.589	0.000
	2	16.02±3.66	14.94–17.11*		
	3	12.13±3.20	11.18–13.08*#		
WSCT persistent error	1	2.24±1.84	1.69–2.79	48.746	0.000
	2	0.20±0.40	0.08–0.32*		
	3	0.26±0.49	0.12–0.41*		
WCST classification	1	5.39±1.14	5.05–5.73	14.082	0.000
	2	4.52±1.03	4.22–4.83*		
	3	4.57±0.93	4.29–4.84*		

Data are mean values ± standard deviation. P[a] values for comparison among three groups (before HAART, after 6 months of HAART, and after 12 months of HAART). *, P<0.05 (compared with before HAART); #, P<0.05 (compared with 6 months of HAART). Group 1, without HAART, Group 2, 6 months of HAART, and Group 3, 12 months of HAART. CI, confidence interval; HAART, highly active antiretroviral therapy; WCST, Wisconsin Card Sorting Test.

use, may contribute to post-HAART results.

In conclusion, our findings show that DTI may be an impersonal imaging modality for assessing the efficacy and neurotoxicity of HAART in HAND-positive patients. Starting HAART may halt the structural deterioration of the WM; however, prolonged HAART could worsen the WM injury, emphasizing the importance of optimal HAART duration. DTI and NP tests may be used as markers for real-time dynamic monitoring efficacy and neurotoxicity of HAART, and this may optimize treatment strategies for HAND-positive patients.

Acknowledgments

The authors thank Prof. Nanning Wu from the Fourth People's Hospital of Nanning for supplying the patients used in this study. We are incredibly grateful to the editors and reviewers.

Funding: Guangxi Science and Technology Department Key Research and Development Programs supported this work (No. AB16380201), Youth Science Foundation of Guangxi Medical University (No. GXMUYSF201532), and International Communication of Guangxi Medical University Graduate Education.

Footnote

Reporting Checklist: The authors have completed the MDAR reporting checklist. Available at http://dx.doi.org/10.21037/atm-20-6342

Data Sharing Statement: Available at http://dx.doi.org/10.21037/atm-20-6342

Conflicts of Interest: All authors have completed the ICMJE uniform disclosure form (available at hhttp://dx.doi.org/10.21037/atm-20-6342). The authors have no conflicts of interest to declare.

Ethical Statement: The authors are accountable for all aspects of the work in ensuring that questions related to the accuracy or integrity of any part of the work are appropriately investigated and resolved. All procedures performed in this study involving human participants were in accordance with the Declaration of Helsinki (as revised in 2013). This study was approved by the Ethics Committee of Wuming Hospital of Guangxi Medical University (No. FSWM2020-126). All patients signed informed consent forms.

References

1. Frew PM, Lutz CS, Ofotokun I, et al. Geospatial mapping to identify feasible HIV prevention and treatment strategies that target specific settings. Ann Transl Med 2018;6:59.
2. Zhao T, Wei B, Long J, et al. Cognitive disorders in HIV-infected and AIDS patients in Guangxi, China. J Neurovirol 2015;21:32-42.
3. Valcour V, Chalermchai T, Sailasuta N, et al. Central nervous system viral invasion and inflammation during acute HIV infection. J Infect Dis 2012;206:275-82.
4. Heaton RK, Franklin DR, Ellis RJ, et al. HIV-associated neurocognitive disorders before and during the era of combination antiretroviral therapy: differences in rates, nature, and predictors. J Neurovirol 2011;17:3-16.
5. Valcour V, Sithinamsuwan P, Letendre S, et al. Pathogenesis of HIV in the central nervous system. Curr HIV/AIDS Rep 2011;8:54-61.
6. Lohse N, Hansen AB, Gerstoft J, et al. Improved survival in HIV-infected persons: consequences and perspectives. J Antimicrob Chemother 2007;60:461-3.
7. Sanford R, Fellows LK, Ances BM, et al. Association of Brain Structure Changes and Cognitive Function With Combination Antiretroviral Therapy in HIV-Positive Individuals. JAMA Neurol 2018;75:72-9.
8. Sanford R, Fernandez Cruz AL, Scott SC, et al. Regionally Specific Brain Volumetric and Cortical Thickness Changes in HIV-Infected Patients in the HAART Era. J Acquir Immune Defic Syndr 2017;74:563-70.
9. Ku NS, Lee Y, Ahn JY, et al. HIV-associated neurocognitive disorder in HIV-infected Koreans: the Korean NeuroAIDS Project. HIV Med 2014;15:470-7.
10. Vivithanaporn P, Heo G, Gamble J, et al. Neurologic disease burden in treated HIV/AIDS predicts survival: a population-based study. Neurology 2010;75:1150-8.
11. Spudich S. HIV and neurocognitive dysfunction. Curr HIV/AIDS Rep 2013;10:235-43.
12. Clifford DB. HIV-associated neurocognitive disease continues in the antiretroviral era. Top HIV Med 2008;16:94-8.
13. Shah A, Gangwani MR, Chaudhari NS, et al. Neurotoxicity in the Post-HAART Era: Caution for the Antiretroviral Therapeutics. Neurotox Res 2016;30:677-97.
14. Ma Q, Vaida F, Wong J, et al. Long-term efavirenz use is associated with worse neurocognitive functioning in HIV-infected patients. J Neurovirol 2016;22:170-8.
15. Antinori A, Arendt G, Becker JT, et al. Updated research nosology for HIV-associated neurocognitive disorders. Neurology 2007;69:1789-99.
16. Hill-Briggs F, Dial JG, Morere DA, et al. Neuropsychological assessment of persons with physical disability, visual impairment or blindness, and hearing impairment or deafness. Arch Clin Neuropsychol 2007;22:389-404.
17. Oh SW, Shin NY, Choi JY, et al. Altered White Matter Integrity in Human Immunodeficiency Virus-Associated Neurocognitive Disorder: A Tract-Based Spatial Statistics Study. Korean J Radiol 2018;19:431-42.
18. Tang Z, Liu Z, Li R, et al. Identifying the white matter impairments among ART-naïve HIV patients: a multivariate pattern analysis of DTI data. Eur Radiol 2017;27:4153-62.
19. Corrêa DG, Zimmermann N, Doring TM, et al. Diffusion tensor MR imaging of white matter integrity in HIV-positive patients with planning deficit. Neuroradiology 2015;57:475-82.
20. Li RL, Sun J, Tang ZC, et al. Axonal chronic injury in treatment-naïve HIV+ adults with asymptomatic neurocognitive impairment and its relationship with clinical variables and cognitive status. BMC Neurol 2018;18:66.
21. Bell RP, Barnes LL, Towe SL, et al. Structural connectome differences in HIV infection: brain network segregation associated with nadir CD4 cell count. J Neurovirol 2018;24:454-63.
22. Strain JF, Burdo TH, Song SK, et al. Diffusion Basis Spectral Imaging Detects Ongoing Brain Inflammation in Virologically Well-Controlled HIV+ Patients. J Acquir Immune Defic Syndr 2017;76:423-30.
23. Ackermann C, Andronikou S, Saleh MG, et al. Early Antiretroviral Therapy in HIV-Infected Children Is Associated with Diffuse White Matter Structural Abnormality and Corpus Callosum Sparing. AJNR Am J Neuroradiol 2016;37:2363-9.
24. Thurnher MM, Castillo M, Stadler A, et al. Diffusion-tensor MR imaging of the brain in human immunodeficiency virus-positive patients. AJNR Am J Neuroradiol 2005;26:2275-81.
25. Stubbe-Drger B, Deppe M, Mohammadi S, et al. Early microstructural white matter changes in patients with HIV:

a diffusion tensor imaging study. BMC Neurol 2012;12:23.
26. Li J, Wu G, Wen Z, et al. White Matter Development is Potentially Influenced in Adolescents with Vertically Transmitted HIV Infections: A Tract-Based Spatial Statistics Study. AJNR Am J Neuroradiol 2015;36:2163-9.
27. Hoare J, Fouche JP, Phillips N, et al. Clinical associations of white matter damage in cART-treated HIV-positive children in South Africa. J Neurovirol 2015;21:120-8.
28. Budde MD, Xie M, Cross AH, et al. Axial diffusivity is the primary correlate of axonal injury in the experimental autoimmune encephalomyelitis spinal cord: a quantitative pixelwise analysis. J Neurosci 2009;29:2805-13.
29. Mac Donald CL, Dikranian K, Bayly P, et al. Diffusion tensor imaging reliably detects experimental traumatic axonal injury and indicates approximate time of injury. J Neurosci 2007;27:11869-76.
30. Song SK, Sun SW, Ramsbottom MJ, et al. Dysmyelination revealed through MRI as increased radial (but unchanged axial) diffusion of water. Neuroimage 2002;17:1429-36.
31. Zhu T, Zhong J, Hu R, et al. Patterns of white matter injury in HIV infection after partial immune reconstitution: a DTI tract-based spatial statistics study. J Neurovirol 2013;19:10-23.
32. Sun SW, Liang HF, Trinkaus K, et al. Noninvasive detection of cuprizone induced axonal damage and demyelination in the mouse corpus callosum. Magn Reson Med 2006;55:302-8.
33. Smurzynski M, Wu K, Letendre S, et al. Effects of central nervous system antiretroviral penetration on cognitive functioning in the ALLRT cohort. Aids 2011;25:357-65.
34. Robertson KR, Su Z, Margolis DM, et al. Neurocognitive effects of treatment interruption in stable HIV-positive patients in an observational cohort. Neurology 2010;74:1260-6.
35. Marra CM, Zhao Y, Clifford DB, et al. Impact of combination antiretroviral therapy on cerebrospinal fluid HIV RNA and neurocognitive performance. Aids 2009;23:1359-66.
36. Cysique LA, Vaida F, Letendre S, et al. Dynamics of cognitive change in impaired HIV-positive patients initiating antiretroviral therapy. Neurology 2009;73:342-8.
37. Wang B, Liu Z, Liu J, et al. Gray and white matter alterations in early HIV-infected patients: Combined voxel-based morphometry and tract-based spatial statistics. J Magn Reson Imaging 2016;43:1474-83.
38. Ragin AB, Wu Y, Gao Y, et al. Brain alterations within the first 100 days of HIV infection. Ann Clin Transl Neurol 2015;2:12-21.
39. Peluso MJ, Meyerhoff DJ, Price RW, et al. Cerebrospinal fluid and neuroimaging biomarker abnormalities suggest early neurological injury in a subset of individuals during primary HIV infection. J Infect Dis 2013;207:1703-12.

Cite this article as: Zhao T, Chen J, Fang H, Fu D, Su D, Zhang W. Diffusion tensor magnetic resonance imaging of white matter integrity in patients with HIV-associated neurocognitive disorders. Ann Transl Med 2020;8(20):1314. doi: 10.21037/atm-20-6342

